Physica Scripta

PAPER • OPEN ACCESS

Shuttlecock velocity decay after smash and slice shots in badminton

To cite this article: Eric Collet 2026 *Phys. Scr.* **101** 125007

IOP Publishing Phys. Scr. 101 (2026) 125007 https://doi.org/10.1088/1402-4896/ae5361

Physica Scripta

OPEN ACCESS

RECEIVED
12 January 2026

REVISED
1 March 2026

ACCEPTED FOR PUBLICATION
17 March 2026

PUBLISHED
26 March 2026

PAPER

Shuttlecock velocity decay after smash and slice shots in badminton

Eric Collet[1,2,*]

[1] Univ Rennes, CNRS, IPR (Institut de Physique de Rennes)—UMR 6251, 35000 Rennes, France
[2] Institut Universitaire de France (IUF), 75231 Paris, France
[*] Author to whom any correspondence should be addressed.

E-mail: eric.collet@univ-rennes.fr

Keywords: badminton, smash, velocity, drag force, time-of-flight

Supplementary material for this article is available online

Abstract

This paper reports on the decay in shuttlecock velocity after smash and slice shots performed by elite and international players, based on the analysis of videos captured on a badminton court with high-speed cameras. For a fast smash, the trajectories of feather shuttlecocks show an exponential decay in velocity and an exponential increase in time-of-flight with distance, in accordance with the equation of motion of a shuttlecock subjected to high drag. The initial speed, which can exceed 500 km h^{-1}, is typically reduced by half every ≈ 3.35 m, depending on the physical parameters of the shuttlecock characterized by a speed index. The videos show that plastic shuttlecocks, which are more resistant than feather shuttlecocks, deform at high speeds. The resulting decay of their drag coefficient with increasing speed makes them unsuitable for high-level play. The study also shows that the spin induced by the slice shots of left-handed players or the reverse slice shots of right-handed players slows the shuttlecock down.

1. Introduction

The smash and slice in badminton are tactical shots, usually played from the back of the court, that often score a point. The smash, hit with power and speed, is also a source of fantasy making badminton the fastest sport in the world: P. Tan set the women's record for fastest hit at 438 km h^{-1}, while S. Rankireddy set the men's record at 565 km h^{-1}. Numerous studies have focused on the particular trajectories of shuttlecocks, which result from the strong aerodynamic drag experienced by these light ($\approx$5 g) and elongated ($\approx$7 cm) particles [1–8]. This drag is essential for keeping the shuttlecock within the confines of the court, as it strongly decreases the velocity of the shuttlecock [9–16]: an initial velocity of $\simeq$240 km h^{-1} (67 m s^{-1}) can decay within $\simeq$0.6 s to $\simeq$25 km h^{-1} (6.9 m s^{-1}).

The speed of the shuttlecock depends on the energy transfer between the player, the racket and the shuttlecock, as underlined by diverse bio-mechanical studies [17–22].

This article presents a quantitative analysis of the trajectories and velocity decay of feather and plastic shuttlecocks after smash shots performed by international and elite players. The effect of the shuttlecock's physical parameters, in particular its mass, is also discussed. These can be adapted on demand to ensure similar playing conditions depending on atmospheric conditions on the planet. The effect of slice and reverse-slice shots on velocity decay is also analysed, for both right- and left-handed players. Some tactical conclusions are discussed, based on experimental and theoretical results. Considering the expected readership, the choice is made to use both the popular velocity unit (km/h) and the metric unit (m/s).

2. Method

A Phantom Miro 3a10 high-speed camera was used on the badminton court to capture high frame rate videos (3000 fps) of shuttlecock trajectories using wide shots or close-ups. The resolution of the videos was maximized

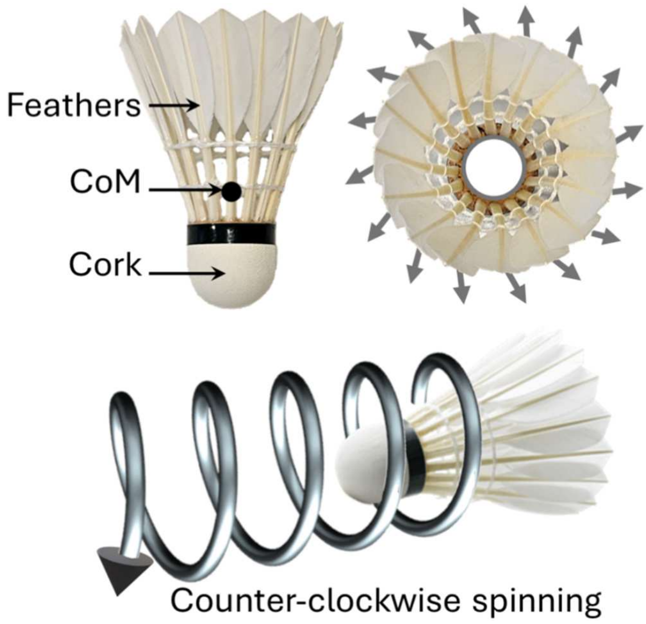

Figure 1. Structure of a feathered shuttlecock. The air flow on the 16 feathers (arrows) induces a natural counter-clockwise spinning.

to 1280 × 800 pixels. A Canon camera was also used, with a capture frame rate set to 500 fps (1920 × 1080 pixels). The shots were performed on court by elite national and international players. Single-shot videos were captured during the French international badminton championships 2025 (IFB) in Rennes. During another dedicated session, 4 players (left-hander male and female, and right-hander male and female) made few smashes, slice or reverse-slice shots. Tracker [23, 24] a free Java video analysis tool, was used to track shuttlecock trajectories and extract speed or time-of-flight curves.

3. Drag force and shuttlecock's speed index

Figure 1 shows the structure of feather shuttlecocks. The centre of mass (CoM) is on the shuttlecock symmetry axis, close to the cork. Feather shuttlecocks do not exhibit mirror symmetry and are chiral bodies [25]. Due to the way the 16 feathers are placed into the cork, the airflow on the feathers is responsible for the natural counter-clockwise spinning of these projectiles as they propagate through the air.

The aerodynamics of shuttlecocks was studied in several papers, based on wind tunnel measurements, video analysis or simulations [1–8, 13, 15, 26, 27]. The equation of motion of a shuttlecock was given in many papers and here we use:

$$m\frac{d\vec{V}}{dt} = m\vec{g} + \vec{F_D} \tag{1}$$

where $\vec{g}$ is gravity, m is the mass of the shuttlecock, $\vec{V}$ its velocity and $\vec{F_D}$ the drag force antiparallel to $\vec{V}$. $\vec{F_D}$ depends on the air density ρ, the cross-section of the shuttlecock (πR^2) with radius R and drag coefficient C_D. The equation reaches:

$$m\frac{d\vec{V}}{dt} = m\vec{g} - \frac{C_D}{2}\pi R^2 \rho V\vec{V} \tag{2}$$

Peastrel *et al* studied the terminal velocity of a shuttlecock in vertical fall [28], where gravity accelerates the shuttlecock, which increases the drag force until weight and drag force balance each other. Then, the projectile reaches its terminal velocity $\vec{V_T}$ in free fall. The velocity is then constant $\left(\frac{d\vec{V}}{dt} = 0\right)$:

$$V_T = \sqrt{\frac{2mg}{C_D \rho \pi R^2}} = A\frac{\sqrt{m}}{R} \tag{3}$$

The typical values for $m = 5.25$ g, $\rho = 1.2$ kg m^{-3}, $\pi R^2 = 35$ cm^2 and $C_D = 0.6$, give a terminal velocity $V_T \approx 24$ km h^{-1} (or 6.5 m s^{-1}).

On earth, ρ changes with various parameters, such as atmospheric pressure, altitude, temperature or humidity. Higher air density causes more drag, which strongly affects V_T and the flying distance of the shuttlecock. In order to ensure similar playing conditions across different locations around the world, the parameters

Table 1. Terminal velocity V_T measured for shuttlecocks with different speed index, mass m and radius R and calculated C_D.

Speed index	AS20 76	AS20 77	AS20 78	Mavis 300
m (g)	5.10(2)	5.25(2)	5.45(2)	5.30(5)
R (cm)	3.35(5)	3.35(5)	3.35(5)	3.30(2)
V_T (m/s)	6.19(2)	6.34(2)	6.48(2)	6.05(2)
$V_T R/\sqrt{m}$	2.90(5)	2.93(5)	2.94(5)	2.49(5)
C_D	0.62(1)	0.61(1)	0.60(1)	0.67(1)

of the shuttlecocks (mass, radius and/or C_D) are adapted to atmospheric conditions. The badminton world federation (BWF) uses shuttlecocks with different 'speed index' ranging from 75 for slower shuttlecocks to 79 for faster shuttlecocks.

Table 1 shows the evolution of V_T measured for a plastic (Mavis 300) and feather shuttlecocks Yonex AS20 with speed indexes from 76 to 78. The drag coefficients C_D, calculated from equation (3) and given in table 1 are in good agreement with values previously reported [1–4, 7, 9–11, 13, 14, 16, 26, 29]. For shuttlecocks with the same C_D, equation (3) predicts that $V_T R/\sqrt{m}$ should be constant. Table 1 shows that, within the experimental uncertainties, it is the case for the AS20 used here. The Mavis 300 has a different shape and C_D, making direct comparisons more difficult.

4. Exponential decay of the shuttlecock velocity

4.1. Theoretical decay of the shuttlecock velocity

Let's consider a shuttlecock reaching an initial velocity of 500 km h^{-1}, as often reported in competition. Since the drag force F_D at $V_T \approx 25$ km h^{-1} equals weight in free fall, and since $F_D \propto V^2$, the drag force is about 400 times larger than weight after such a smash stroke at 500 km h^{-1}. Weight is then negligeable at high speed. The equation of motion is then simplified, with the drag force antiparallel to the velocity:

$$m\frac{dV}{dt} = -\frac{1}{2}\rho\pi R^2 C_D V^2 \tag{4}$$

By introducing the infenitesimal travel $dr = Vdt$ of the shuttlecock during dt, (4) can be rewritten:

$$\frac{dV}{V} = -\frac{1}{2m}\rho\pi R^2 C_D dr \tag{5}$$

and integrating (5) gives:

$$V(r) = V_0^{Theo}\exp\left(-\frac{\rho\pi R^2 C_D}{2m}r\right) = V_0^{Theo}\exp\left(-\frac{r}{L}\right) \tag{6}$$

Equation (6) describes the exponential decay with the distance r of the velocity of a point mass shuttlecock, for an initial theoretical velocity V_0^{Theo}. $L = \frac{2m}{\rho\pi R^2 C_D}$ is called the aerodynamic length and a typical value is $L \approx 4.5$ m (2). For general readers, it is convenient to use $L_{1/2} = ln(2)L$, which is the characteristic velocity halving distance.

Figure 2 shows the theoretical velocity decay from equation (6), for $L_{1/2}$= 3.35 m and $V_0^{Theo} = 500$ km h^{-1} (139 m s^{-1}) at the backline of the badminton court. The length of the court is 13.4 m = 4 $L_{1/2}$, which means that the shuttlecock velocity is divided by 4 (125 km h^{-1}) at the net and by16 ($\approx$31 km h^{-1}) at the opposite backline of the court, which approaches V_T. Then the weight can't be neglected anymore to accurately describe the trajectory. The range of validity of equation (6) to describe the trajectory is therefore questionable. Figure 3(a) shows the trajectory of the centre of mass (CoM) of shuttlecock Yonex AS50 77 after a fast smash, performed in the downward direction to hit the court (by T. Jr Popov during the IFB 2025).

The (x,y) trajectory is extracted from the video analysis, where x is the horizontal distance along the long court axis and y is altitude of the shuttle. The diverse temporal (0.3–2 ms) and spatial resolution and the tracking precision (2–5 mm / pixel) used provided a relatively accurate measurement of the parameters of different trajectories (x, y, r, t). The dispersion of the experimental velocity data on the different $V(r)$ curves is due to the limitations imposed by the fps versus pixel resolution set-up, with an accuracy ranging from $\approx$3 km h^{-1} for high speed and close-ups shots with high spatial resolution to $\approx$15 km h^{-1} for low speed and wide shots with low spatial resolution.

The trajectory in figure 3(a) of the CoM is fairly close to a linear trajectory (black line). The y coordinate is affected by gravity during the time-of-flight of 300 ms. However, after 9.5 m and a time of flight of 300 ms, the y

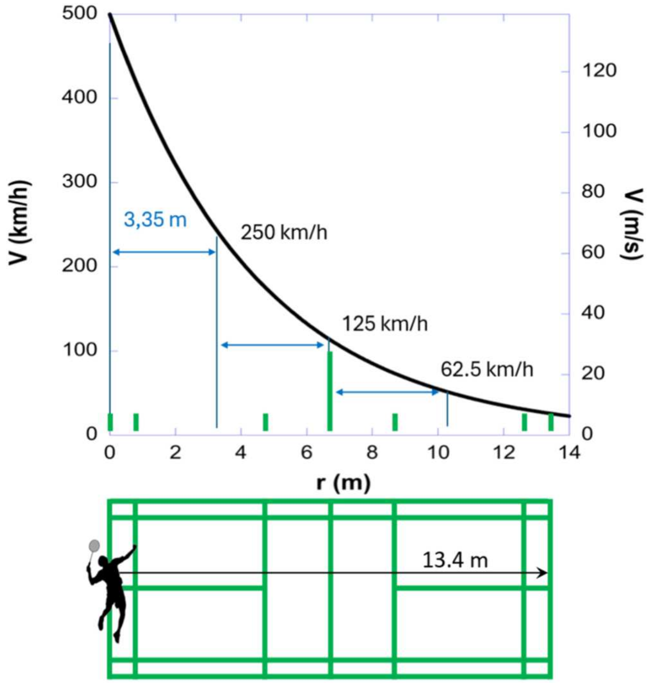

Figure 2. Theoretical exponential velocity decay of the shuttlecock along the court, for an initial speed of V_0^{Theo}=500 km h^{-1} (≈139 m s^{-1}) and a velocity halving distance $L_{1/2} \approx 3.35$ m.

coordinate deviates only by 10 cm from the linear trajectory. This is less than the displacement of a free-falling object in gravity during a time-of-flight of 300 ms, $\frac{1}{2}gt^2 = 45\ cm$. Indeed, the shuttlecock propagating in the air is not a free-falling object, due to the important drag force.

Figure 3(b) shows the measured velocity decay $V(r)$ of the shuttlecock's CoM with the distance r from the point of impact with the racket. The fit of $V(r)$ with the exponential law (black curve, equation (6)) is in fairly good agreement with the experimental data and gives an initial velocity $V_{0CoM}^{Fit} = 379(1)$ km h^{-1} and aerodynamic length $L_{77}^{Fit} = 4.73(2)$ m for the AS50 77. The error bars for the initial speed and aerodynamic length are extracted from the least-squares fitting procedures of the $V(r)$ data curves with equation (6). L_{77}^{Fit} is close to the theoretical value, but it depends on the shuttlecock characteristic and the potential damage it sustains during gameplay, which alters the drag force.

Figure 4(a) shows the (x,y) trajectory for a slower smash. The initial speed of ≈180 km h^{-1} decays to ≈ 30 km h^{-1} after 9 m (figure 4(b)). Both curves show a good agreement with the simple linear trajectory and exponentially decaying velocity, up to ≈6 m where $V \approx 50$ km h^{-1}. After, the trajectory is affected by the effect of the gravity: the (x,y) trajectory deviates from linear. In addition, the velocity tends towards a limit value close to V_T and not towards 0, as the shuttlecock falls. This sets the limits of validity of the model in equation (6). When the velocity of the shuttlecock is higher than $2V_T$, the drag force is about 4 times larger than weight, which can be neglected in equation (1). Equation (6) is reasonably valid for $V > 2V_T$. Overall, it is reasonable to consider that equation (6) is relatively accurate to describe the shuttlecock trajectory after a smash with a high initial velocity higher than 300 km h^{-1} and up to the first 10 m.

4.2. The velocity of what? Cork versus centre of mass (CoM)

Given that a badminton shuttlecock is not a point object, one might wonder which velocity should be measured. Should we consider the initial speed of the CoM (V_{OCoM}) or the one of the cork (V_{OCork})? The CoM is a natural choice when considering the shuttlecock as a point object. However, BWF rules consider the point of impact of the cork on the court to award points, and it is the speed of the cork that is measured to set the record for the fastest badminton hit.

Figure 5 shows the evolution of both velocities after a smash stroke, performed by A.S. Rasmussen (IFB 2025 with a Yonex AS50 77, video psae6561supp1.mp4) . The fit of the velocity of the CoM with an exponential law (blue curve) fairly agrees with the data and gives an initial velocity $V_{0CoM}^{Fit} = 396(1)$ km h^{-1} and an aerodynamic length $L_{77}^{Fit} = 4.17(2)$ m.

The speed of the cork strongly deviates from the exponential law during the first meter. This is due to the flipping process, as the orientation of the shuttle changes from almost vertical to almost horizontal along the final trajectory. The measured initial speed of the cork in figure 5 is much higher ($V_{0Cork}^{meas} = 451(1)$ km h^{-1}) than

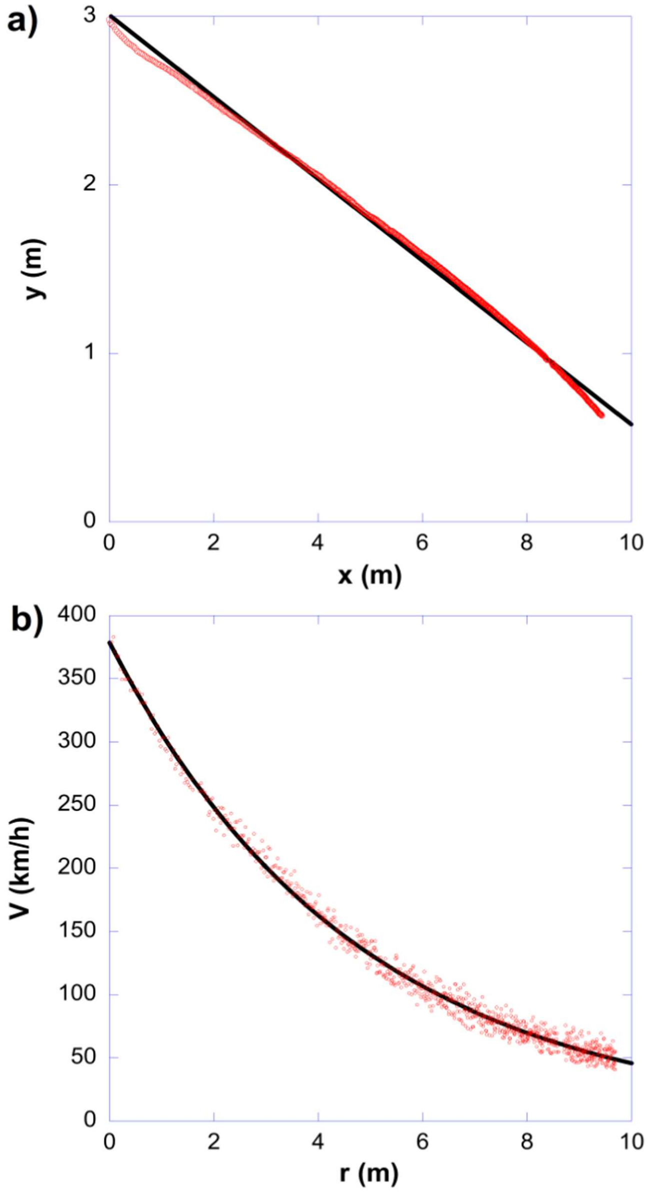

Figure 3. (a) The shuttlecock (x,y) trajectory for a fast smash is almost linear: x is the coordinate along the court and y the altitude. (b) CoM velocity decay with distance *r* for the smash shot (dots). The black line is the exponential fit with equation (6).

the one of the CoM ($V_{0CoM}^{meas} = 396(1)$ km h^{-1}). Finaly, both velocities converge (within the experimental error bar) once the axis of the shuttle is aligned along the trajectory.

Figure 6 shows a closer inspection of the velocity of the CoM of the shuttle, monitored over the first 2.5 m (shot by C.-L. Wang during the IFB 2025, video psae5361supp2.mp4). The shuttlecock undergoes a huge acceleration during the first 10 cm after the impact with the racket. The velocity increases from 21 km h^{-1} to 399 km h^{-1} within 1.3 ms, which corresponds to an acceleration of about 8000 g! The maximal velocity measured for the CoM (V_{0CoM}^{meas}= 399 km h^{-1}) at 10 cm from the initial impact is slightly higher than the value from the fit at this position (396 km h^{-1}), while the extrapolation of the fit at the point of impact slightly overestimate the speed ($V_{0CoM}^{Fit} = 409$ km h^{-1}). Considering that the velocity decays by ≈1 km h^{-1} every cm, a precise determination of V_{0CoM}^{Fit} requires determining the point of impact with an accuracy of ≈ 1 cm.

In addition, figure 6 evidences a damped oscillation of the CoM velocity around the simple exponential decay fit (red curve). The correlation between the chronograph and the $V(r)$ curve highlights that the deceleration is higher when the shuttlecock axis is not aligned along the trajectory. The orientation of the shuttlecock with respect to the velocity is measured by the angle φ (figure 5). Cohen *et al* explained this flipping process of the shuttle [2] as the drag forces on the feathers and on the cork align the shuttlecock axis along the velocity. Equation (1) and (6) describe the translation of the centre of mass facing a drag force associated with a constant drag coefficient C_D, which corresponds to the normal situation when the shuttlecock axis points along the velocity (φ = 0, situation 3 in figure 5). However, the angle φ of the shuttlecock axis with velocity undergoes

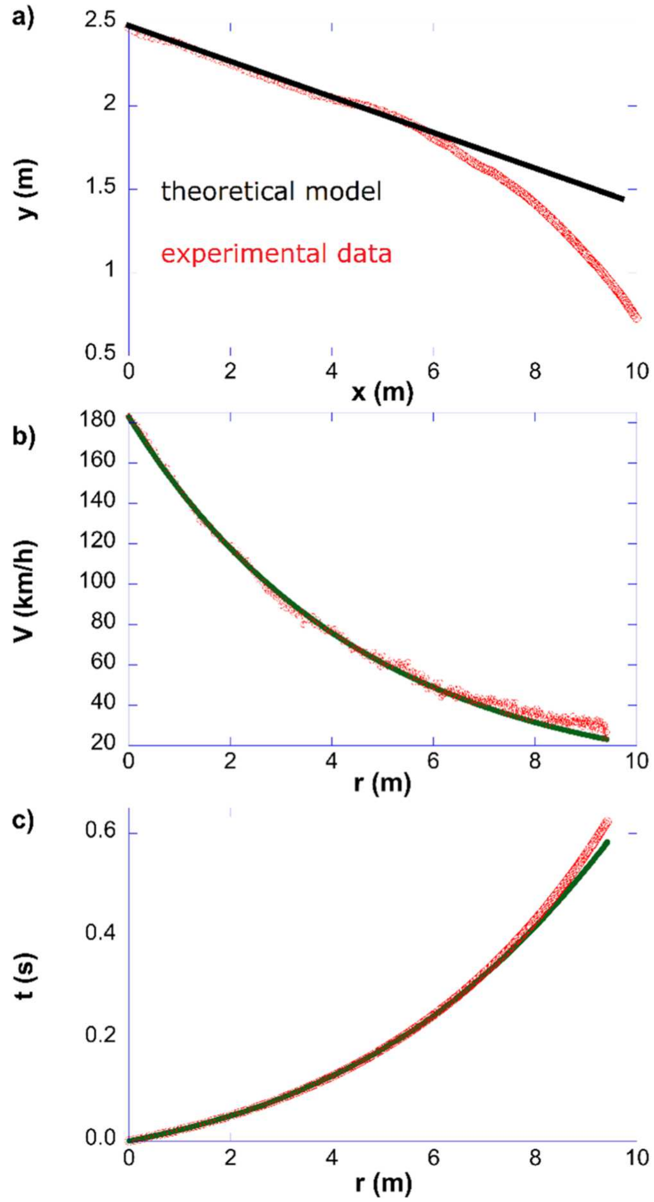

Figure 4. (a) Shuttlecock trajectory for a slow smash shot. (a) (x,y) coordinates. (b) Velocity decay with the distance *r* from the smash. (c) Time *versus* distance r. The experimental data (red) agree with equation (6) for speed higher than 50 km h^{-1} ($\approx 2V_T$).

significant damped oscillation just after smash, which affect the drag coefficient. Cohen *et al* have measured the evolution of the drag coefficient of a shuttlecock in a wind tunnel as a function of its orientation φ [2]. C_D changes from 0.6 when the shuttlecock is aligned along the velocity ($\varphi = 0°$) to 0.9 for $\varphi = 70°$. The damped oscillating velocity of the CoM (figure 6) around the exponential decay, exhibiting more or less important deceleration as φ oscillates, is therefore associated with the damped oscillation of C_D along the trajectory. The inset in figure 6 shows that the exponential fit deviates by ≈8 km h^{-1} for the initial speed, and this deviation is damped within ≈1 m. Overall, the fitted V_{0CoM}^{Fit} is a relevant parameter.

4.3. 'Fast' versus 'slow' shuttlecocks

How does the change in the shuttlecock speed index affects the $V(r)$ curve? Figure 7 shows the velocity decay measured after different smash shots for AS20 shuttlecocks with speed index 76 and 78. These have similar shapes but different masses (table 1) and therefore different aerodynamic lengths. The least-squares refinement fits of the experimental $V(r)$ curves in figure 7 with equation (6) gives similar initial velocities for both shots (≈320(2) km h^{-1}) and a longer aerodynamic length for the speed index 78 ($L_{78}^{Fit} = 4.49(1)$ m) compared to 76 ($L_{76}^{Fit} = 4.23(1)$ m). These values, increasing with mass, are in good agreement with the theoretical values $L_{78}^{Theo} = 4.29$ m $L_{76}^{Theo} = 4.02$ m, calculated for $\rho = 1.2$ kg.m^{-3}. High-speed index shuttlecocks have lower deceleration and higher average speeds than low-speed ones.

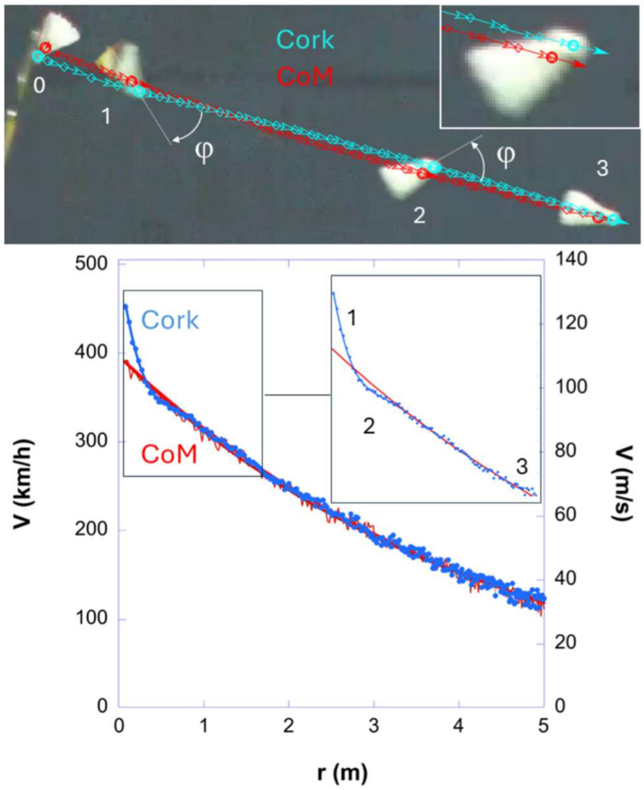

Figure 5. Positions, paths and velocities (arrows) of the CoM (red) and cork (blue) of the shuttlecock, altered by its orientation (φ) with respect to the CoM velocity from almost perpendicular (0) to colinear (3). After the smash, the cork is faster (1) or slower (2) than the CoM. Both velocities are equal for $\varphi = 0$.

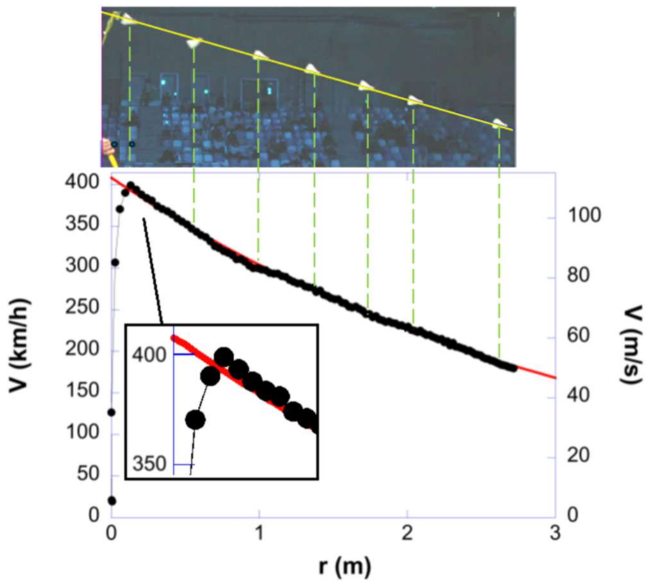

Figure 6. Deviation of the velocity of the CoM from the exponential law (red fit). The deceleration is larger when the shuttle axis is not aligned along the trajectory (yellow line).

4.4. Plastic shuttlecocks

The main problem with feather shuttlecocks used in competition is that they are easily damaged during play. They therefore need to be replaced frequently to maintain their flight characteristics. During the last decades synthetic shuttlecock emerged, made from plastics, with overwhelming advantages in durability, cost-effectiveness, and consistency in recreational play [15]. Plastic shuttlecocks, whose skirts are mainly made of

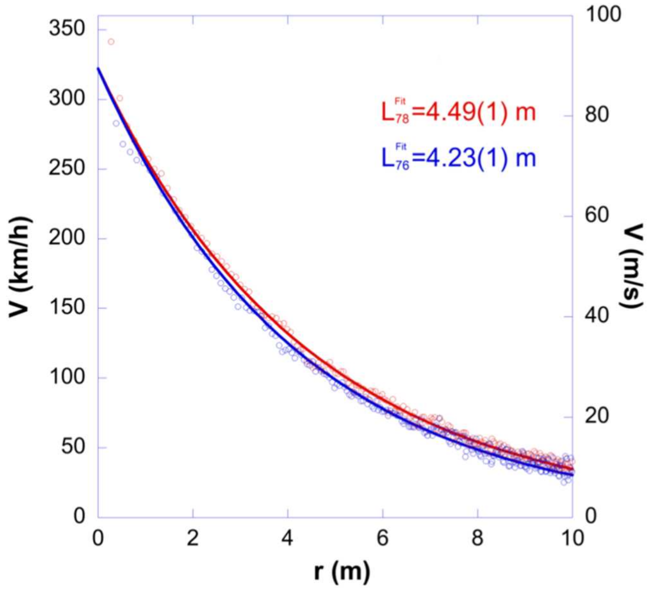

Figure 7. Velocity decay after smash shot for Yonex AS20 shuttlecocks. The aerodynamic length is higher for the shuttlecock with fast speed index 78 ($L_{78}^{Fit} = 4.49(1)$ m) compared to the one with a slow index 76 ($L_{76}^{Fit} = 4.23(1)$ m).

nylon, are becoming increasingly popular in non-competitive badminton, as their flexibility gives them greater durability. However, this flexibility comes at the cost of inferior flight quality compared to feather shuttlecocks.

The terminal velocity of the plastic shuttlecock is lower than the one of the feathers. Based on the data in table 1, the aerodynamic length for the Mavis 300 is $L_{300}^{Theo} = 3.90$ m. Figure 8 shows the velocity decay measured for the Mavis 300 shuttlecock, for different initial velocities. The fits of the $V(r)$ curves with equation (6) allows extracting the evolution of the aerodynamic length. For $V_{0CoM}^{Fit} = 239$ km h^{-1}, $L_{300}^{Fit} = 4.03(1)$ m is in good agreement with L_{300}^{Theo}. However, the aerodynamic length increases with increasing initial speed, up to $L_{300}^{Fit} = 4.31(1)$ m for $V_{0CoM}^{Fit} = 304$ km h^{-1}. Several studies have shown that the drag coefficient of synthetic shuttlecocks decreases with increasing speed, due to the deformation of the skirt with the air pressure at high speed [3–5, 10, 13, 26]. The air flow reduces the cross-section of the plastic shuttlecock by a factor of 2 at 50 m s^{-1} compared to the cross section at rest. A recent computational study [30] confirmed how the cross-sectional area of the skirt decreases with an increase in flight speed, leading to a significant reduction in the drag compared to that for an undeformed shuttlecock. This study also evidenced that beyond a certain speed, the deformation of the skirt assumes a non-axisymmetric shape with a significant increase in its rate of deformation with speed.

Video psae5361supp3.mp4 and figure 9 show that the air pressure on the flexible nylon skirt deforms the plastic shuttlecock as it flies, from an initial shape with 16-fold symmetry to square or triangular shapes after smash. Both the reduction in cross-section and the change of shape contribute to an overall decrease the drag force, and therefore an increase of aerodynamic length with initial speed. This global evolution of the drag force along the trajectory is complex to describe. Video psae5361supp3.mp4 and figure 9 show that as the shuttlecock slows down and the air pressure on the skirt decreases and the initial 16-fold symmetry shape is recovered within ≈3 meters. However, the cross section is still reduced at 36 km h^{-1} [10]. The results in figure 8 and 9, measured on a badminton court, confirm previous experimental and theoretical analyses concerning the variation in drag coefficient with the initial velocity. Plastic shuttlecocks are therefore hard to control due to the flexibility of their skirt, which affect the drag force.

5. Effect of slice and reverse slice on velocity decay

The slice shot is another tactical technique, known for causing the shuttle to spin and altering the angle of return. Kitta and Cohen conducted experiments on feather shuttlecock [1, 2] and concluded that the shuttlecock with natural spin experiences a marginally larger drag compared to shuttle without spin. A recent study explained why the slice shot of the left-handed player (LH) is more efficient than the slice shot of the right-handed player (RH) [25], due to the chiral nature of a shuttlecock. The helical arrangement of the feathers is responsible for its natural counter-clockwise rotation as it propagates through the air (figure 1).

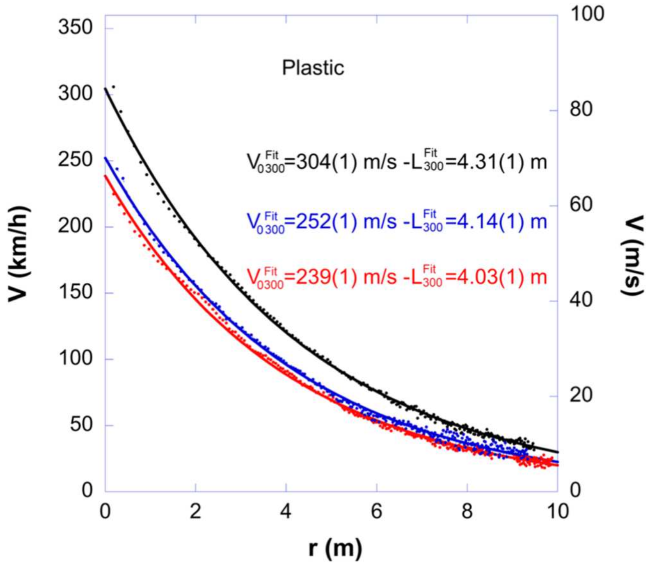

Figure 8. Velocity decay after smash shot for plastic Yonex Mavis 300 shuttlecocks for different initial velocities V_0. The fit of the $V(r)$ curves with equation (6) shows that the aerodynamic length increases with initial velocity.

Figure 9. Deformation of the skirt of a plastic shuttlecock at high speed after impact with racket, with triangular or square shapes depending on initial velocity. As the shuttlecock slows down and spins, the initial shape is recovered within ≈3 m.

Video psae5361supp4.mp4 shows that the slice shots performed by right-handers induce a natural counter-clockwise spinning. On the contrary, the slice shots performed by left-handers induce an opposite clockwise spinning: the air flow on the feathers then stops the rotation and the shuttlecock, which finally spins naturally counter-clockwise. Reversely, the reverse slice shots performed by LH induce a natural counter-clockwise spinning, while the reverse slice shots performed by RH induce a clockwise to counter-clockwise spinning.

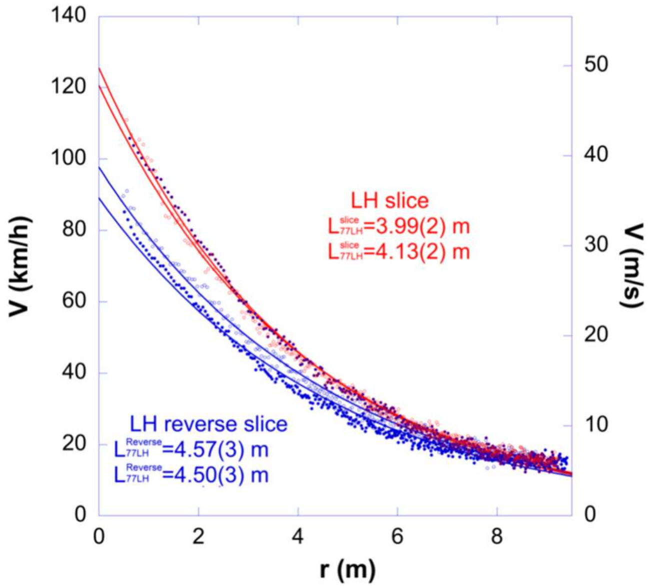

Figure 10. Comparison of the velocity decay of shuttlecocks (AS20) for left-hander (LH) slice ($\langle L^{Slice}_{77LH}\rangle \approx 4.06$ m) and LH reverse slice ($\langle L^{Reverse}_{77LH}\rangle \approx 4.53$ m).

Figure 10 compares the decrease in shuttlecock (AS20 77) velocity after slice shots and reverse slice shots for a left-handed player.

The fits of the $V(r)$ curves with equation (6) show that the speed decreases more rapidly for the left-handed slice shot than for the left-handed reverse slice shot, as characterized by the shorter average aerodynamic length for the two LH slices ($\langle L^{Slice}_{77LH}\rangle \approx 4.06$ m compared to the one for the two LH reverse slices ($\langle L^{Reverse}_{77LH}\rangle \approx 4.53$ m). Figure 11 shows that the situation is reversed for RH players (AS20 76 shuttlecock). The fit gives a longer aerodynamic length ($L^{Slice}_{76RH} \approx 4.19(2)$ m) for the RH slice shot than for average one for the two RH reverse slices ($\langle L^{Reverse}_{76RH}\rangle \approx 3.21(2)$ m). Compared to a natural counter-clockwise rotation induced by a RH slice or a reverse LH slice, the opposite clockwise rotation induced by a LH slice or a reverse RH slice results in a more effective slowing down of the shuttlecock. Indeed, these last induce a clockwise to counter-clockwise spinning of the shuttlecock (video psae5361supp4.mp4). This means that the kinetic energy of the shuttlecock is therefore transferred to rotation energy due to the air drag on the helical arrangement of the feathers. Describing this complex energy transfer between a translating and spinning object in a fluid, is a real challenge and it will be subject to future studies.

6. Lessons learned

This study shows that it is possible to describe with a good accuracy the velocity change of a fast badminton shuttlecock after smash or slice shots as an exponential decay with distance. The aerodynamic properties of the shuttlecocks, described through their speed index, allows adjusting the shuttlecock to the local atmospheric conditions. The speed decay is very fast as velocity is typically halved every ≈3.35 m, with important consequences in the game, which are of great interest for players or coaches.

Figure 2 shows that the velocity decay is important within the first meter. A smash at 500 km h^{-1} from the backline is equivalent to a smash at ≈400 km h^{-1} shot one meter in front of the backline. It is therefore of tactical importance for a player in a defensive position, who has to lift the shuttlecock and who will have to face the smash of the opponent, to push the opponent at the very back of the court.

This point is even more interesting in terms of time-of-flight of the shuttlecock, which is found by integrating equation (6):

$$t(r) = \frac{L}{V_0}\left(\exp\left(\frac{r}{L}\right) - 1\right) \tag{7}$$

Figure 12 shows the measured dependence of the time-of-flight with distance $t(r)$ for a smash performed with a AS20 78. The fit of the data (green curve) with equation (7) gives $V_0^{Fit} = 300(1)$ km h^{-1} for this shot, and the aerodynamic length $L^{Fit}_{78} = 4.48(2)$ m is again in good agreement with the result for another shot in figure 7. Figure 12 shows that the time of flight for an initial speed of 300 km h^{-1} increases from ≈440 ms to travel over

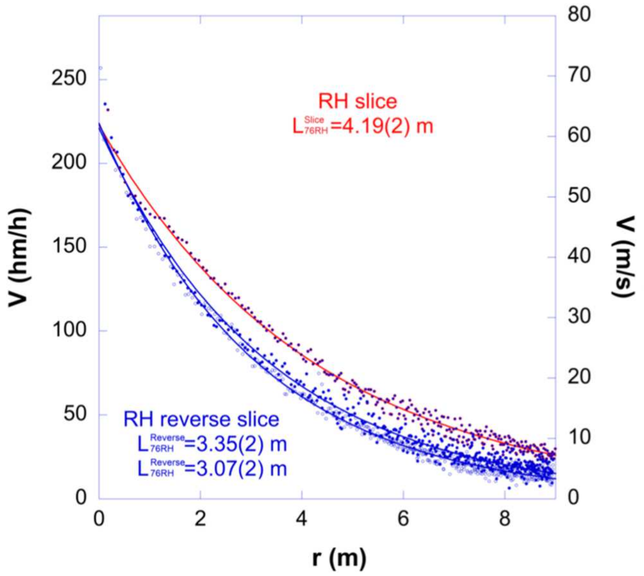

Figure 11. Comparison of the velocity decay of shuttlecocks (AS20) for right-hander (RH) slice ($\langle L^{Slice}_{76RH}\rangle \approx 4.19(2)$ m) and RH reverse slice ($\langle L^{Reverse}_{76RH}\rangle \approx 3.21(2)$ m).

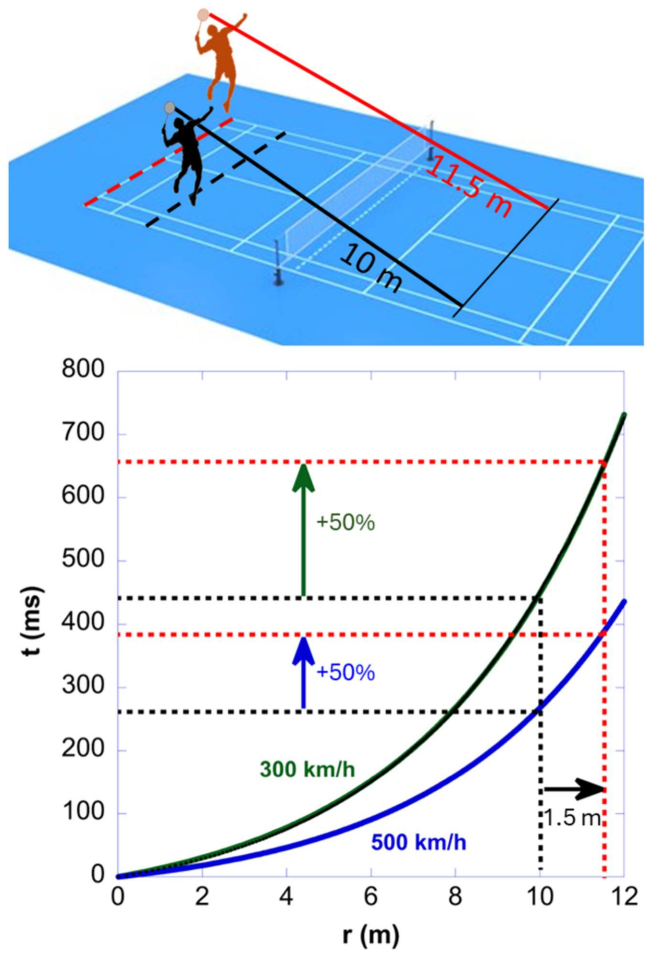

Figure 12. Fit (green) of the time-of-flight of a AS20 78 shuttlecock (black dots) after a smash shot for an initial velocity of $\approx$300 km h^{-1} and theoretical curve (blue) for an initial velocity of $\approx$500 km h^{-1} Blue. The time-of-flight increases by $\approx$+50% for a smash of 11.5 m *versus* 10 m.

10 m to ≈660 ms to travel over 11.5 m. This also highlights the importance of pushing the smasher towards the back of the court. Indeed, for a given initial velocity, increasing the distance travelled from 10 m to 11.5 m increases the reaction time to defend the smash by 50%, as also shown with the calculated curve (blue, figure 12) for an initial speed of 500 km h^{-1}. Equation (7) is valid for a smash with high initial speed (> 300 km h^{-1}), as the experimental data and the theoretical curve perfectly match. This is no more the case for slower smash (<200 km h^{-1}) after 6 m, as shown in figure 4(c).

7. Conclusion

The fitting methods of the speed decay versus distance $V(r)$ curves based on equation (6), or of the time-of-flight versus distance $t(r)$ curves based on equation (7), allows for extracting both the initial speed of the centre of mass of the shuttlecock and its aerodynamic length with a good accuracy for fast smashes. This study confirms that the aerodynamic length increases with shuttlecock's speed index. It also shows that the opposite rotation of the shuttlecocks induced by the LH slice or RH reverse slice decreases the aerodynamics length. This is due to a complex energy transfer between the kinetic energy and the rotation energy of the shuttlecock, mediated by the air drag on the feathers.

For sustainability reasons, the BWF initiative to transition from traditional feather shuttlecocks to synthetic-feather shuttlecocks has introduced equipment changes that could impact gameplay. The flight characteristic of plastic shuttlecocks with an aerodynamic length depending on the initial velocity, makes it difficult to control their trajectory. For this reason, plastic shuttlecock, which have interesting longevity, cannot fully replicate the precise flight behaviour of a high-quality natural feather shuttle. As new synthetic shuttlecocks made of carbon appeared recently on the market [31], it will be interesting to compare the flight characteristics and speed decay of this new generation of shuttlecocks with traditional feathered shuttles, which are currently the benchmark for flight quality.

Acknowledgments

E.C. would like to thank B. Kersaudy, A. Lièvre, E. Gautier and C. Allaire, the players who participated in this study, and M. Dureault, K. Nakamura and A. Gauthier for technical support. The author also thanks the BWF, the FFBad and especially C. Grandamas for providing access to the court during IFB 2025 in Rennes. E.C. would also like to thank Gillian Clark and Steen Pedersen for fruitful discussions.

Data availability statement

The data cannot be made publicly available upon publication because they are not available in a format that is sufficiently accessible or reusable by other researchers. The data that support the findings of this study are available upon reasonable request from the authors. https://doi.org/10.5281/zenodo.18142286 [32].

References

[1] Kitta S, Hasegawa H, Murakami M and Obayashi S 2011 Aerodynamic properties of a shuttlecock with spin at high reynolds number *Procedia Engineering* **13** 271–7
[2] Cohen C, Texier B D, Quéré D and Clanet C 2015 The physics of badminton *New J. Phys.* **17** 063001
[3] Chan C M and Rossmann J S 2012 Badminton shuttlecock aerodynamics: synthesizing experiment and theory *Sports Eng.* **15** 61–71
[4] Verma A, Desai A and Mittal S 2013 Aerodynamics of badminton shuttlecocks *J. Fluids Struct.* **41** 89–98
[5] Mehta R C 2023 Aerodynamics of Sport Balls, Badminton Shuttlecock and Javelin *Scholars Journal of Engineering and Technology* **11** 4–10
[6] Chen L M, Yh Fau P, Chen Y-J and Chen Y J A Study of Shuttlecock's Trajectory in Badminton (Print) 1303–2968 (https://jssm.org/volume08/iss4/cap/jssm-08-657.pdf)
[7] Texier B D, Cohen C, Quéré D and Clanet C 2012 Shuttlecock dynamics *Procedia Engineering* **34** 176–81
[8] Goff J E 2013 A review of recent research into aerodynamics of sport projectiles *Sports Eng.* **16** 137–54
[9] Texier B D, Cohen C, Dupeux G, Quéré D and Clanet C 2014 On the size of sports fields *New J. Phys.* **16** 033039
[10] Cohen C, Darbois Texier B, Quéré D and Clanet C 2011 Physics of badminton shuttlecocks *Aerodynamics* **1** M10.008
[11] Phomsoupha M and Laffaye G 2014 Shuttlecock velocity during a smash stroke in badminton evolves linearly with skill level *Comput. Meth. Biomech. Biomed. Eng.* **17** 140–1
[12] Hubbard M 1997 Editor Spin dynamics of the badminton shuttlecock (https://semanticscholar.org/paper/Spin-dynamics-of-the-badminton-shuttlecock-Hubbard/c91f1ac2c90af115dcfe904c6079afb5f22d42b6)
[13] Cooke A J 1999 Shuttlecock aerodynamics *Sports Eng.* **2** 85–96
[14] Cooke A 2002 Computer simulation of shuttlecock trajectories *Sports Eng.* **5** 93–105
[15] Woo T, Alam F and Kootsookos A 2024 Scientific development of badminton shuttlecocks *Sustainability and Sports Science Journal* **2** 149–65
[16] Zhou L 2024 Aerodynamic characteristics and trajectory analysis of badminton shuttlecocks *Acta Bioeng. Biomech.* **26** 29–37

[17] Phomsoupha M and Laffaye G 2015 The science of badminton: game characteristics, anthropometry, physiology, visual fitness and biomechanics *Sports Medicine* **45** 473–95
[18] Li S, Zhang Z, Wan B, Wilde B and Shan G 2017 The relevance of body positioning and its training effect on badminton smash *Journal of Sports Sciences* **35** 310–6
[19] Ramasamy Y, Usman J, Sundar V, Towler H and King M 2024 Kinetic and kinematic determinants of shuttlecock speed in the forehand jump smash performed by elite male Malaysian badminton players *Sports Biomechanics* **23** 582–97
[20] Ramasamy Y, Wei Y M, Towler H and King M 2025 Intra-Individual Variation in the Jump Smash for Elite Malaysian Male Badminton Players *Applied Sciences* **15** 844
[21] McErlain-Naylor S A, Towler H, Afzal I A, Felton P J, Hiley M J and King M A 2020 Effect of racket-shuttlecock impact location on shot outcome for badminton smashes by elite players *Journal of Sports Sciences* **38** 2471–8
[22] Aguinaldo A L and Escamilla R F 2022 Induced power analysis of sequential body motion and elbow valgus load during baseball pitching *Sports Biomechanics* **21** 824–36
[23] Brown D and Cox A J 2009 Innovative Uses of Video Analysis *The Physics Teacher* **47** 145–50
[24] https://opensourcephysics.github.io/tracker-website/
[25] Collet E 2024 Left- versus right-handed badminton slice shots: opposite spinning of the chiral shuttlecock and Magnus effect *C.R. Phys.* **25** 1–15
[26] Alam F, Chowdhury H, Theppadungporn C and Subic A 2010 Measurements of aerodynamic properties of badminton shuttlecocks *Procedia Engineering* **2** 2487–92
[27] Reistad N 2022 The jerk and the vertical fall of a shuttlecock *Eur. J. Phys.* **43** 055804
[28] Peastrel M, Lynch R and Armenti A 1980 Terminal velocity of a shuttlecock in vertical fall *Am. J. Phys.* **48** 511–3
[29] Nakagawa K, Hasegawa H, Murakami M and Obayashi S 2012 Aerodynamic Properties and Flow Behavior for a Badminton Shuttlecock with Spin at High Reynolds Numbers *Procedia Engineering* **34** 104–9
[30] Zala D, Dechiraju H and Mittal S 2024 Computational analysis of the fluid–structure interactions of a synthetic badminton shuttlecock *Phys. Fluids* **36** 015113
[31] Tan K J Z *et al* 2025 Impact of a new synthetic shuttlecock on badminton performance and player perception *Proc. of the Institution of Mechanical Engineers, Part P: Journal of Sports Engineering and Technology*
[32] Collet E 2026 Shuttlecock velocity decay after smash and slice shots in badminton *Zenodo* (https://doi.org/10.5281/zenodo.18142286)